The University of Tehran Press

Pollution

Print ISSN: 2383-451X
Online ISSN: 2383-4501

https://jpoll.ut.ac.ir/

Magnesium, Zinc, and Iron Co-doped Titanium Dioxide: A Novel Visible-Light Sonophotocatalyst for Enhanced Photocatalytic degradation of methyl orange

Helia Hassanzadeh Bavojdan | Mohammad Ghorbanpour✉ | Roghayeh Shahriari

Faculty of Chemical and Petroleum Engineering, University of Tabriz, Tabriz, Iran

Article Info

Article type:
Research Article

Article history:
Received: 4 October 2024
Revised: 19 February 2025
Accepted: 17 July 2025

Keywords:
Co-doping
Sono-photocatalytic activity
Wastewater treatment

ABSTRACT

This study reports the successful synthesis of Mg, Fe, and Zn Co-doped TiO2 nanoparticles via a rapid heating technique, exhibiting enhanced sono-photocatalytic activity under both visible and UV light irradiation. Various characterization methods, including X-ray diffraction (XRD), scanning electron microscopy (SEM), energy dispersive X-ray analysis (EDX), and diffuse reflectance UV-vis spectroscopy (UV-DRS), were employed to assess the produced materials. The codoping process led to a significant reduction in the band-gap energy from 3.16 eV to 2.60 eV, facilitating the absorption of visible light and improving the generation of reactive oxygen species. The sono-photocatalytic activity of the Co-doped TiO2 nanoparticles was evaluated by degrading methyl orange solutions, achieving a remarkable degradation efficiency of 48.7% under visible light and 60.1% under UV light. The combined effect of ultrasound and light irradiation synergistically boosted the photocatalytic activity, outperforming each method individually. The Co-doped TiO2 nanoparticles demonstrated a higher efficiency compared to previous investigations, highlighting their potential as a novel visible-light sonophotocatalyst for environmental remediation applications.

Cite this article: Hassanzadeh Bavojdan, H., Ghorbanpour, M., & Shahriari, R. (2025). Magnesium, Zinc, and Iron Co-doped Titanium Dioxide: A Novel Visible-Light Sonophotocatalyst for Enhanced Photocatalytic degradation of methyl orange. *Pollution*, 11(3), 781-793.
https://doi.org/10.22059/poll.2025.383239.2586

DOI: https://doi.org/10.22059/poll.2025.383239.2586

INTRODUCTION

Titanium dioxide (TiO_2) has gained significant attention as a photocatalyst for breaking down dyes due to its abundance, stability, and non-toxic properties (Akhter et al., 2022). However, its wide band gap of 3.2 eV limits its efficiency in utilizing solar light, as only ultraviolet light can provide enough energy for electron transitions between the valence and conduction bands of TiO_2 (Ghorbanpour and Feizi, 2019). This limitation presents challenges for practical applications. Recent advancements in modifying TiO_2 to enhance its photocatalytic performance under visible light have shown promising results in degrading various organic dyes commonly found in industrial wastewater (Sewnet et al., 2022) Techniques such as incorporating metal dopants and forming hetero-junctions have effectively reduced the band gap of TiO_2, thereby improving its ability to absorb visible light and increase the generation of reactive species (Fagan et al, 2016).

The improvement of photocatalytic activity in TiO_2 through doping is mainly attributed to changes in its electronic structure. When dopants are introduced into TiO_2, they create localized

*Corresponding Author Email: *Ghorbanpour@tabrizu.ac.ir*

energy levels within the band-gap (Na-Phattalung et. al., 2022). This facilitates the absorption of visible light and enhances the excitation and movement of electrons. Notably, the addition of iron has been shown to effectively reduce the band-gap of TiO_2, thereby increasing its ability to absorb light in the visible spectrum (Darwish et al. 2021; Madadi et al., 2018; Madadi et al., 2019). Moreover, iron doping can also impact the crystallinity and surface morphology of TiO_2. The ionic radius of Fe^{3+} (0.64 Å) is similar to that of Ti^{4+} (0.68 Å), allowing Fe^{3+} to replace Ti within the crystal lattice. This substitution promotes the formation of an inter-band level between the conduction band and the valence band edge, which can absorb visible light (Mancuso et al. 2021). Additionally, the inclusion of zinc ions in the TiO_2 structure alters its electronic properties and improves the mobility of charge carriers, essential for efficient photoreactive processes. Zinc doping also enhances the stability and durability of TiO_2 under operational conditions, making it suitable for long-term applications (Liu et al., 2019; Nisar et al., 2024). The incorporation of magnesium ions into the TiO_2 lattice has been shown to significantly enhance the mobility of charge carriers and improve their stability (Ganesan et al., 2024).

In essence, the process of co-doping with iron, magnesium, and zinc effectively modifies the band gap and optimizes the electronic structure, resulting in enhanced light absorption within the visible spectrum. Moreover, co-doping TiO_2 with multiple dopants simultaneously has a significant synergistic effect on photocatalytic performance compared to undoped samples (Ghorbanpour and Feizi 2020; Chen et al., 2023). The introduction of various dopants can create interstitial or substitutional defects that act as electron traps (Xu et al., 2020). Consequently, when TiO_2 is exposed to visible light, these dopants can capture the excited electrons in the conduction band, prolonging their lifetime and improving overall photocatalytic efficiency. This is particularly important for applications such as the degradation of organic pollutants, where increased electron availability can lead to improved degradation rates. Furthermore, the deliberate engineering of TiO_2 through co-doping not only enables the utilization of visible light but also aligns with sustainable practices by utilizing abundant and cost-effective elements. The development of sustainable photocatalysts is crucial for the advancement of technologies aimed at addressing global environmental challenges and meeting energy demands.

The use of a special type of catalyst that responds to visible light and ultrasound has proven to be highly effective in improving the breakdown of various pollutants. When ultrasound is applied, it helps disperse the catalyst particles, improves the movement of substances, and creates reactive molecules through a process called cavitation (Zhang et al., 2019). Combining this ultrasound-assisted catalysis with the light-responsive properties of the catalyst leads to a powerful combined effect that significantly enhances the breakdown of pollutants. This makes it especially useful for real-world applications like treating wastewater and purifying air.

Research on sustainable methods for creating Co-doped TiO_2 has attracted a lot of attention lately. Techniques like sol-gel processes (Cheng et al., 2012; Zhang et al., 2012), hydrothermal synthesis (Luu et al., 2024), and co-precipitation (Luu et al., 2024) have shown promise in producing high-quality nanostructured TiO_2 with tailored properties. In a recent study by Mancuso et al. (2021), a range of tri-doped TiO_2 photocatalysts was successfully synthesized using the sol-gel method. These included Fe-N-P/TiO_2, Fe-N-S/TiO_2, Fe-Pr-N/TiO_2, Pr-N-S/TiO_2, and P-N-S/TiO_2. The researchers then assessed the photocatalytic degradation of thiacloprid under UV-A, visible, and direct solar light exposure. In a separate investigation, Umare et al. (2013) demonstrated that Ga, N, and S co-doped TiO_2 showed enhanced activity under visible light for the degradation of azo dyes. Notably, Maki et al. (2019) achieved the highest dye removal efficiency among various doping configurations by synthesizing Fe-Ce-N tri-doped TiO_2 (Maki et al., 2019). Furthermore, Cheng et al. (2012) developed Fe–N–S tri-doped

TiO_2 through a simple one-step sol–gel process, incorporating ammonium ferrous sulfate in the reaction. These reports indicated satisfactory outcomes, but the processes involved are complex and require precise control across multiple steps. In contrast, this study utilizes a simple, rapid, cost-effective, one-step solid-state heating method. This technique holds significant promise as it involves the incorporation of dopants, including both metals and nonmetals, through high-temperature treatments, enhancing the diffusion of these elements into the TiO_2 lattice. The elevated temperatures not only increase the solubility of the dopants but also impact the crystalline structure, potentially altering the band-gap energy and improving charge carrier dynamics.

This research introduces a straightforward and effective method for synthesizing tri-metallic doped titanium dioxide, which serves as a visible-light activated sonophotocatalyst, thereby improving the photocatalytic degradation of methyl orange. In the current study, methyl orange has been utilized as a model pollutant. Methyl orange is characterized by its azo structures, which are linked to toxicity and potential carcinogenic effects, thereby raising significant health concerns. The occurrence of this compound in industrial wastewater poses risks to public health and aquatic ecosystems, underscoring the necessity for its removal to safeguard environmental integrity (Alalwan et al., 2023; Rehan et al., 2023). The effects of these dopants on the decolorization process of methyl orange solution have been extensively investigated. Additionally, the morphology and microstructure of the produced nanoparticles have been characterized through techniques such as X-ray diffraction (XRD), diffuse reflectance spectroscopy (DRS), and energy-dispersive X-ray (EDX) scanning electron microscopy (SEM).

MATERIAL AND METHODS

All chemicals, including methyl orange, TiO_2, $MgNO_3$, $AgNO_3$, and $ZnCl_2$ were purchased from Merck Co., (Germany) and applied without further purification.

Add properties to all chemicals

Doping

The TiO_2 and suitable amounts of $MgNO_{3,}$ $AgNO_3$, $ZnCl_2$, each constituting 10% W/W of TiO_2, were carefully mixed, milled, and blended to ensure an even distribution of the three compounds within the final mixture. Next, this mixture underwent thermal treatment in a furnace at a temperature of 700°C for 60 minutes. After the process, the synthesized nanoparticles were rinsed thoroughly with distilled water. Following the washing step, the nanoparticles were dried in an oven maintained at 25°C.

Characterization

The samples' morphological characteristics were analyzed using a scanning electron microscope (SEM) model LEO 1430VP from Germany. A Scinco S4100 spectrophotometer from South Korea was utilized for diffuse reflectance UV-visible spectroscopy (DR UV-Vis) over a wavelength range of 200 to 800 nm. For the powder X-ray diffraction (XRD) analysis, a Philips PW 1050 diffractometer from the Netherlands, equipped with a nickel filter and copper

Photocatalytic activity

The nanoparticles' ability to degrade methyl orange (MO) was tested using a combination of ultrasonic waves and light exposure. Initially, the MO aqueous solution (50 ppm, 50 ml) and photocatalyst (1 g/l) mixture was allowed to reach equilibrium in the absence of light for 5 min. Subsequently, the mixture was subjected to irradiation using a 6 W UV lamp and a certain

amount of visible light, while being sonicated in an ultrasonic bath. After certain times of 5, 10, 15, 30, 60 and 90 min, the solution was centrifuged (10000 rpm, 10 min), and the absorbance was measured using a UV-visible spectrophotometer to calculate the degradation percentage. The efficiency of photocatalytic degradation was determined using the formula:

Degradation efficiency (%) = $(A_0 - A) / A_0 * 100$

Where A_0 represents the initial absorbance of the dye solution and A represents the absorbance after irradiation.

RESULTS AND DISCUSSIONS

Characterization

The XRD patterns for both the undoped and Co-doped samples are shown in Figure 1. Both samples exhibit prominent diffraction peaks at around 25.3° and 48.1°, confirming the presence of TiO_2 in its anatase form (samples (Ghorbanpour and Feizi 2020). This suggests the absence of any significant impurity phases. Anatase is considered one of the best structures of titanium dioxide (TiO_2) primarily due to its superior photocatalytic activity compared to other forms like rutile. This increased activity makes anatase particularly effective for applications in photocatalysis, such as in environmental remediation and solar energy conversion. Its tetragonal crystal structure contributes to its unique properties, although it is generally regarded as a metastable form compared to rutile (Peiris et, 2021). However, the results of this study suggest that the co-doping process did not lead to any observable phase transition from anatase to alternative phases, such as rutile. This implies that the doping process either had a minimal influence on the TiO_2 structure or that any newly formed phases are present in such low concentrations that they remain undetectable by the X-ray diffraction method used.

After analyzing the parent samples, it was found that the mean grain size is around 38.3 nm using the Scherrer equation based on the full width at half-maximum of the (101) diffraction peak (2θ = 25.6) for TiO_2 (Zhang et al. 2012). Following the co-doping process, the size increased to 48.1 nm. This increase in size can be linked to the difference in atomic radii between the TiO_2 particles and the zinc elements. The larger atomic size of zinc induces strain within the

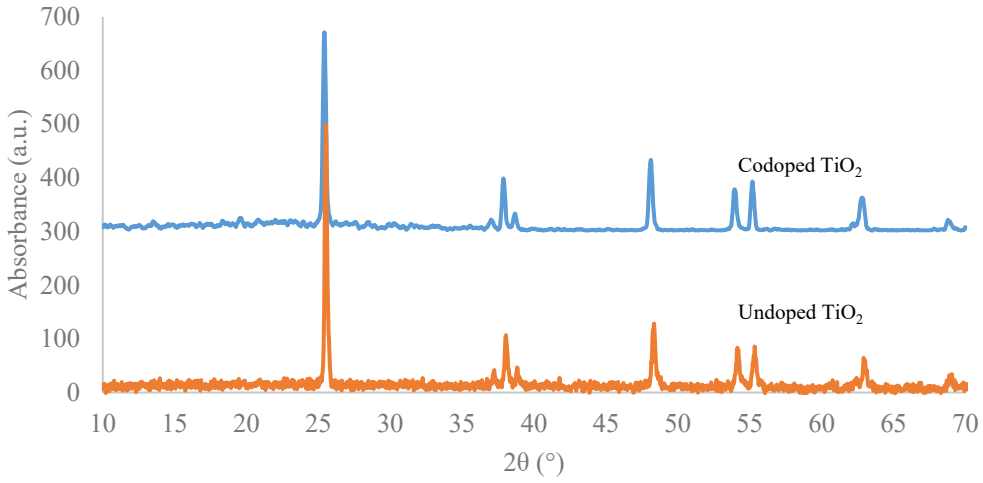

Fig. 1. The XRD patterns of the undoped and Co-doped samples

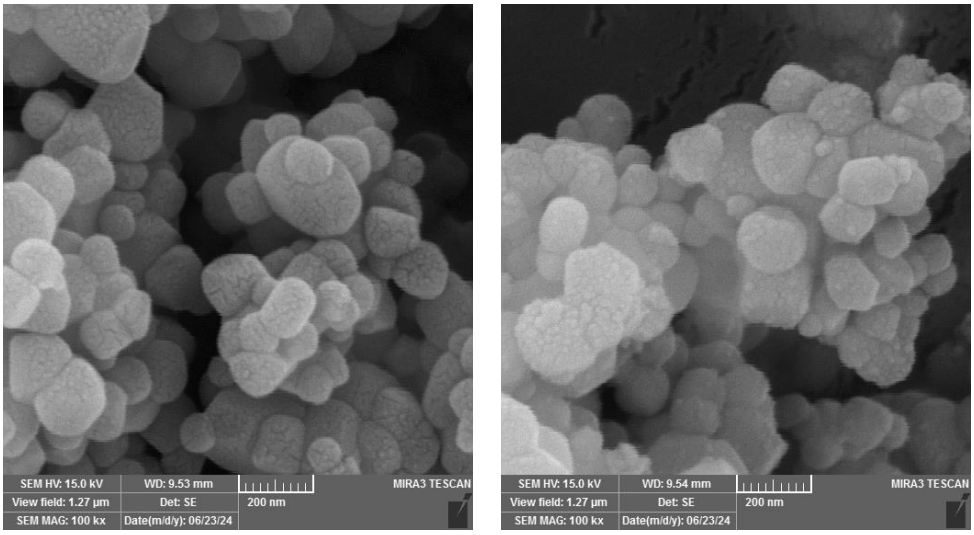

(a) (b)

Fig. 2. The SEM images of the undoped (a) and Co-doped (b) TiO_2

TiO_2 lattice, leading to the agglomeration of smaller crystallites into larger structures (Yihunie, 2024). Additionally, the introduction of iron into the TiO_2 matrix may also result in an increase in crystal size, resulting from the modification of the surface characteristics of the TiO_2 particles by iron doping (Abza et al., 2022). However, it's important to note that the influence of doping on crystal size is complex and may vary based on several factors, including the concentration of the dopant and the method of synthesis.

Upon examining Figure 2, it is evident that both the undoped and Co-doped samples share similar morphologies. The primary nanoparticles display a relatively consistent size and are predominantly spherical in shape. Interestingly, there is no discernible difference in the morphology of pure and co-doped titania. However, it is worth noting that the observed particle size appears to be larger than the XRD results suggest. This disparity can be attributed to the fact that SEM assesses the overall dimensions of a particle, taking into account surface characteristics and agglomerations, whereas XRD evaluates the dimensions of individual crystallites within the particle.

The analysis using EDX was carried out to verify the incorporation of Zn, Fe, and Mg elements onto the surface of TiO_2 after the doping process through heating. As shown in Figure 3a, the TiO_2 spectra display additional peaks after the metal doping, indicating the successful introduction of Zn, Fe, and Mg into the synthesized Co-doped sample. The distinct spectra of the Co-doped TiO_2 demonstrate the presence of Ti, O, Mg, Fe, and Zn elements, with atomic percentages of 23.17%, 74.37%, 1.04%, 0.63%, and 0.79%, respectively. The corresponding weight percentages are 46.02%, 49.33%, 1.05%, 1.46%, and 2.13%. For further investigation, the analysis was also performed on nanoparticles (Figure 3b). This analysis indicated the uniform distribution of Mg, Fe, and Zn elements in the structure of the nanoparticles. This indicates the presence of these elements in the crystal structure of TiO_2 nanoparticles.

The UV–vis spectra shown in Figure 4a depict the absorption profiles of both the undoped and Co-doped samples. These profiles are typical of wide band gap oxide semiconductors and feature a distinct absorption band with a sharp edge, indicating electron transitions from the valence band to the conduction band. The band gap energies are found to be 3.16 eV for the pure sample and 2.60 eV for the Co-doped TiO_2 sample, as indicated in the inset of Figure 4b. Notably, a red shift in the absorption spectra is observed after the doping process. Previous

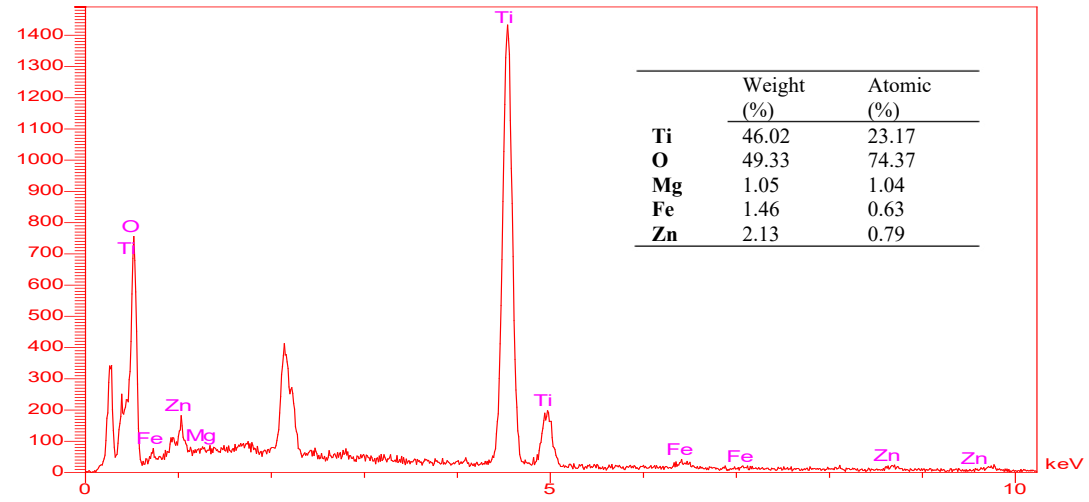

	Weight (%)	Atomic (%)
Ti	46.02	23.17
O	49.33	74.37
Mg	1.05	1.04
Fe	1.46	0.63
Zn	2.13	0.79

(a)

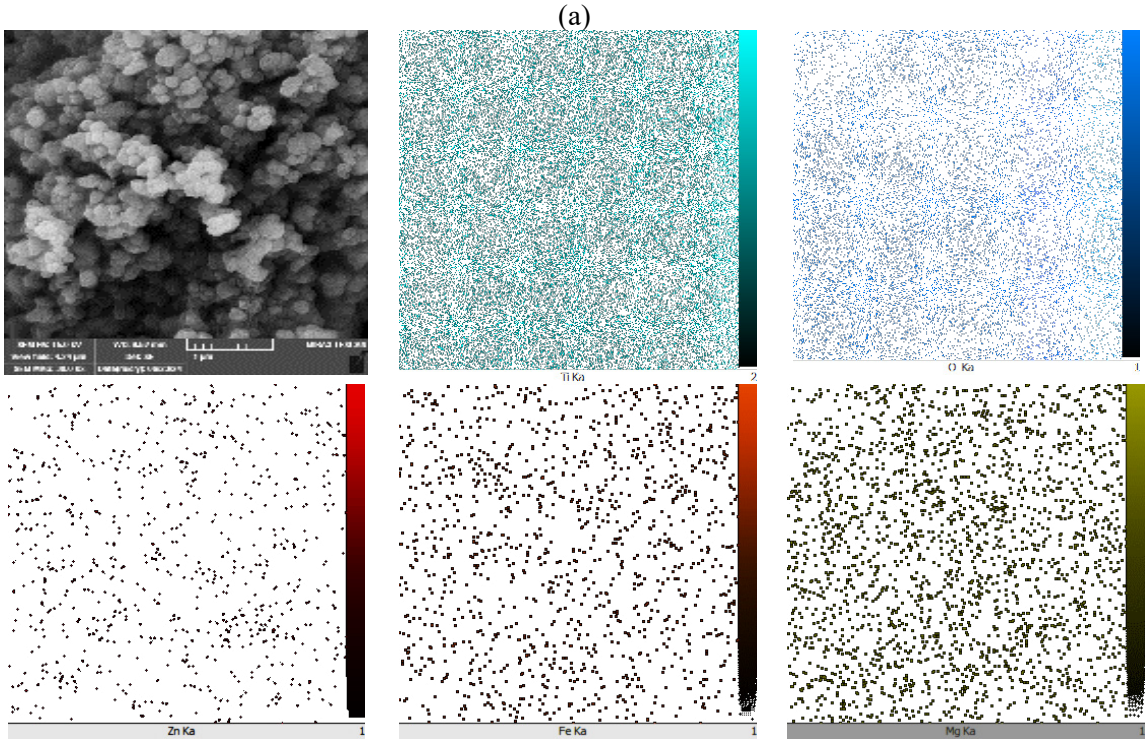

(b)

Fig. 3. EDX spectrum (a) and MAP-EDX (b) of the Co-doped sample

studies have suggested that the red shift is associated with new formed states positioned above the valence band maximum of TiO_2, while the blue shift is primarily attributed to the emergence of oxygen vacancies and the presence of Ti^{3+} in TiO_2 (Dozzi and Selli, 2013). Therefore, it is reasonable to conclude that the incorporation of Fe, Zn, and Mg into the TiO_2 lattice has led to alterations in the crystal structure and electronic characteristics of the tri-doped TiO_2. In previous research, it was found that the band gaps for (Zn,N)-Co-doped TiO_2, Pr-N-S TiO_2 and FeNS Co-doped TiO_2 were reported as 3.02 eV (Mancuso et al, 2021), 2.5 eV (Zhang et al., 2012), and 1.96 eV (Jabbari et al. (2015), respectively.

Photocatalytic activity

The samples were evaluated for their sono-photocatalytic performance by observing

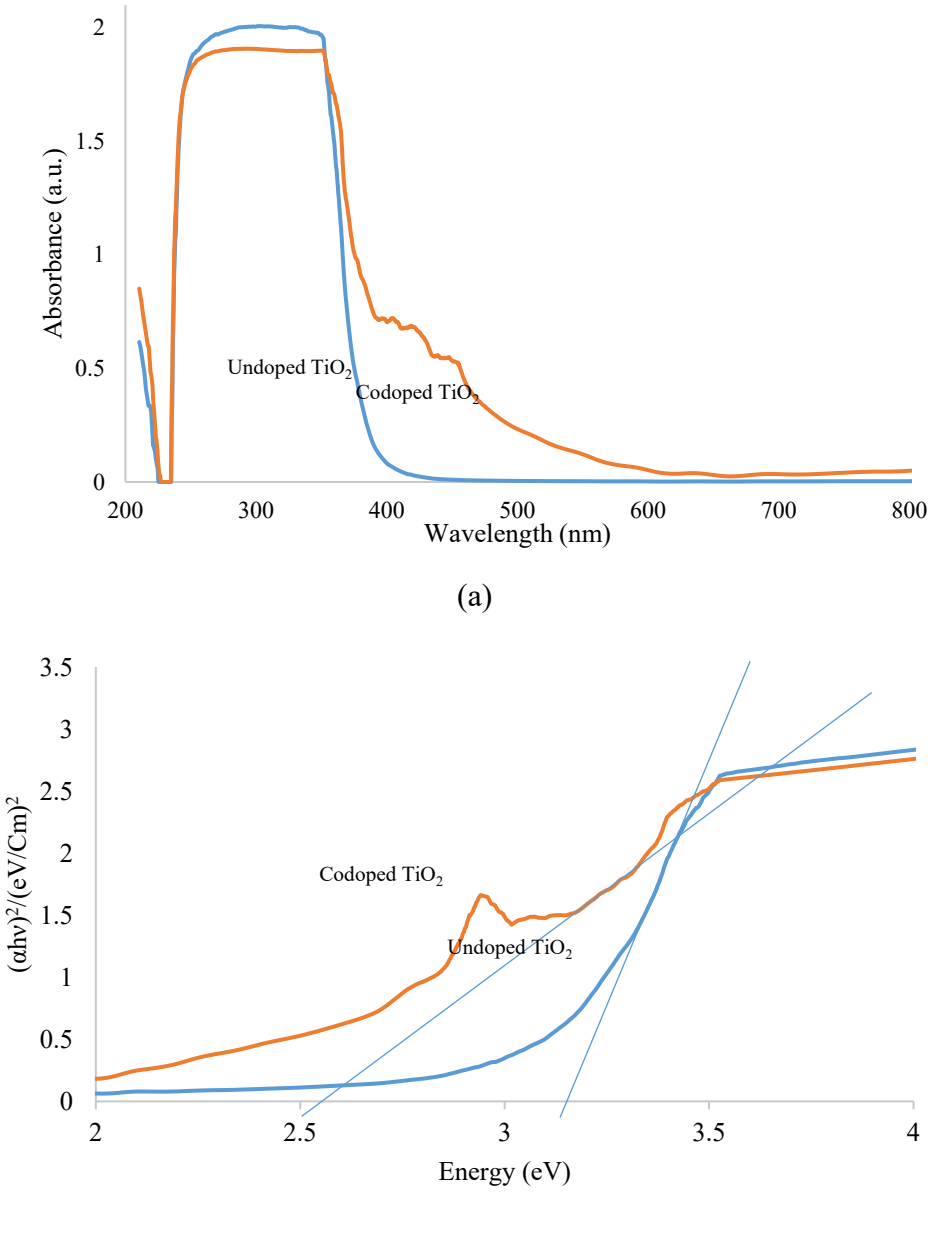

Fig. 4. The UV–vis spectra (a) and band gap (b) of the undoped and Co-doped samples

how they degraded the methyl orange solution. According to Figure 5, the degradation rate of MO was studied in relation to the duration of light and ultrasound irradiation applied to both undoped and co-doped TiO_2 samples. The results depicted in the figure show that co-doping significantly improves the degradation efficiency under both visible (from 12.8% to 48.7%)) and UV (from 19.3% to 60.1%) light conditions. When a semiconductor is exposed to radiation during photoexcitation, electrons (e^-) are shifted from the valence band to the conduction band (figure 6). This process creates vacancies or holes (h^+) in the valence band. The released charge carriers can move to the catalyst's surface, where they can initiate redox reactions with adsorbed species. For instance, the positive holes in the valence band can oxidize hydroxide ions or water molecules at the surface, resulting in the production of hydroxyl radicals ($^{\cdot}OH$). These radicals are potent oxidizing agents with an energy of 2.89 eV and can participate in the oxidation of organic compounds. Simultaneously, electrons in the

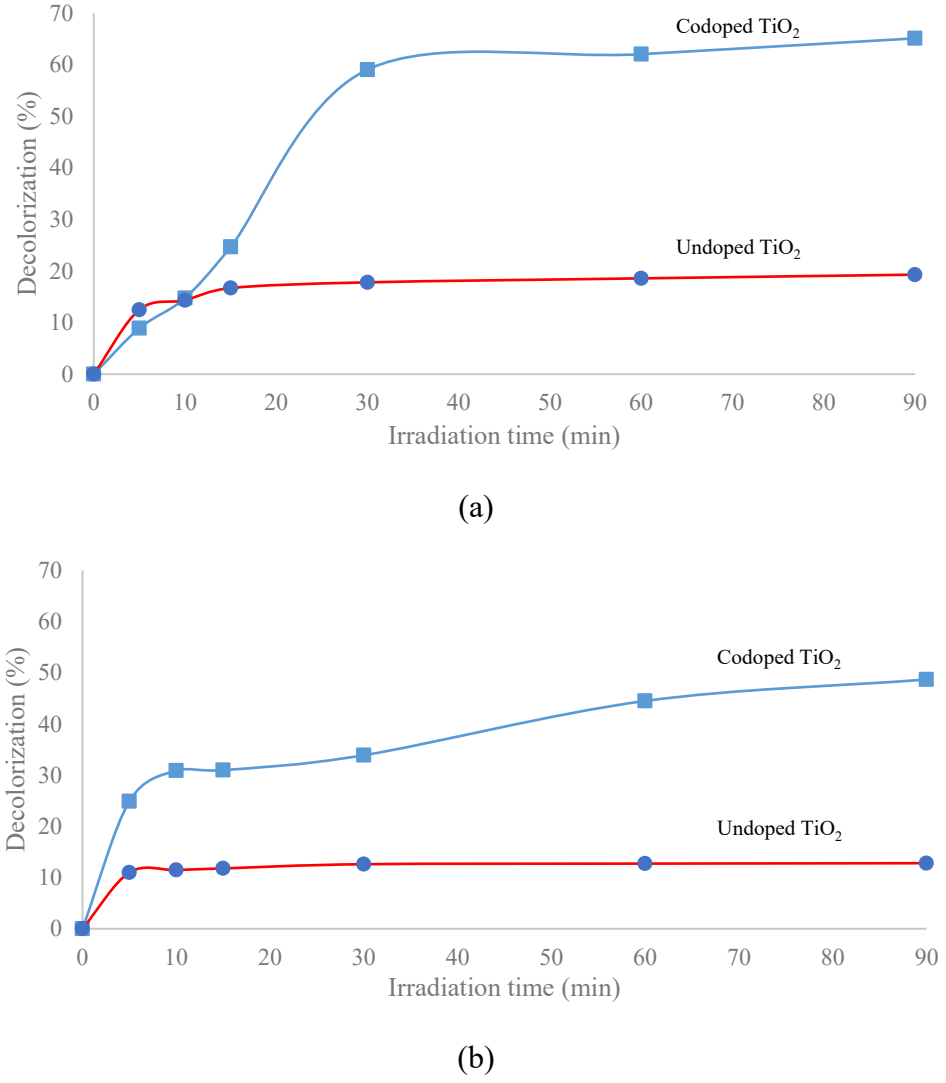

Fig. 5. The sono-photocatalytic activities of undoped and Co-doped TiO_2 under UV (a) and visible (b) light irradiation

conduction band can be rapidly captured by molecular oxygen adsorbed on TiO_2 particles, leading to the generation of superoxide radical anions ($O_2^{\cdot-}$). These anions can further react with protons to form hydroperoxyl radicals ($^{\cdot}OOH$), and subsequent electrochemical reduction can yield hydrogen peroxide. The reactive oxygen species produced through these processes can significantly impact the breakdown of organic pollutants (Kunnamareddy et al., 2018). The co-doping process led to an increase in the diameter and crystallite size of TiO_2, a reduction in the band gap, and an increase in the number of surface active sites available for the adsorption of O_2 molecules and hydroxyl ions. These changes facilitate the breaking of chemical bonds in methyl orange, resulting in the formation of colorless dye molecules. The parent TiO_2 displayed minimal photocatalytic activity when exposed to visible light irradiation, mainly due to its band gap of 3.12 eV, which limits its ability to absorb visible light and generate reactive oxygen species (ROS) necessary for the effective degradation of MO. Co-doping improves the photocatalytic activity of TiO_2 under visible light by reducing the band gap to 2.6 eV, enabling the absorption of visible light and the generation of electron-hole pairs for photocatalytic processes (Gogate, 2020). However, its photocatalytic efficiency remains lower than that observed under UV light for several

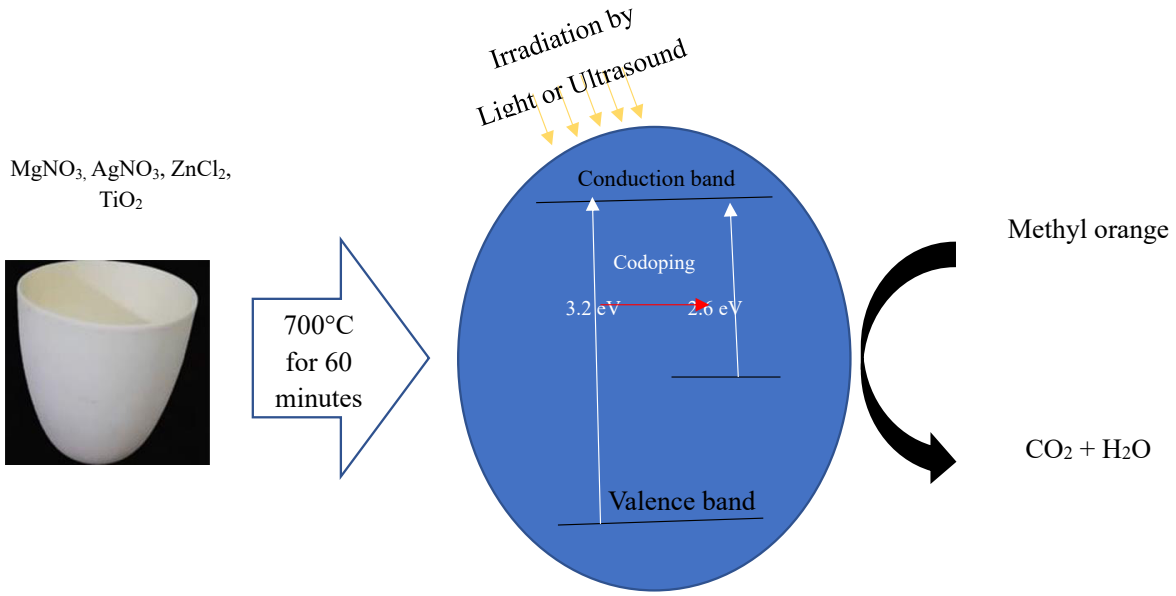

Fig. 6. Schematic of the photocatalytic degradation mechanism of methylene orange

reasons: a) UV light has a higher energy level, which more effectively excites electrons in TiO_2, leading to enhanced photocatalytic activity; b) while doping extends the absorption spectrum of TiO_2 into the visible range, this absorption is still limited compared to that of UV light; and c) the introduction of defects or impurities through doping may adversely impact photocatalytic performance.

The samples we prepared show different levels of degradation under light and ultrasound irradiation, as shown in Figure 7. In the current study, methyl orange has been utilized as a model pollutant (Waliullah et al., 2023). It's worth noting that both methods enhance photocatalytic activity, but they work in distinct ways. When light excites the electrons in the photocatalyst, it helps move them from the valence band to the conduction band, creating electron-hole pairs. Moreover, light exposure can alter the surface properties of the photocatalyst, such as crystallinity or oxidation states, affecting its reactivity and promoting the formation of reactive species like hydroxyl radicals, which boost pollutant degradation. On the other hand, ultrasound enhances photocatalytic activity through cavitation effects, improved mass transfer, surface activation, and particle disaggregation (Gogate, 2020). The combination of ultrasound and light irradiation (UV or visible) synergistically boosts the photocatalytic activity of Co-doped TiO_2, surpassing the efficacy of each method alone. The combined use of silver (Ag) and sulfur (S) has been found to improve the breakdown of methylene blue when exposed to visible light at an intensity of 5.80 mW cm^{-2} (Kunnamareddy et al., 2018). In a study conducted by Zhang et al. (2012), (Zn, N)-co-doped TiO_2 nanoparticles were created using the sol-gel method, achieving an 85% decolorization rate for a 10 mg/l methylene blue solution under 500 W of visible light exposure. Similarly, Jabbari et al. (2015) documented the decolorization of a 10 mg/l methyl orange aqueous solution using In, V-co-doped TiO_2 (0.1 g) under 400 W of visible light. As a result, this current study demonstrates a higher efficiency compared to many previous investigations. It is important to note that the initial concentration of the dye in this study was 50 ppm, which is significantly greater than that used in the aforementioned studies.

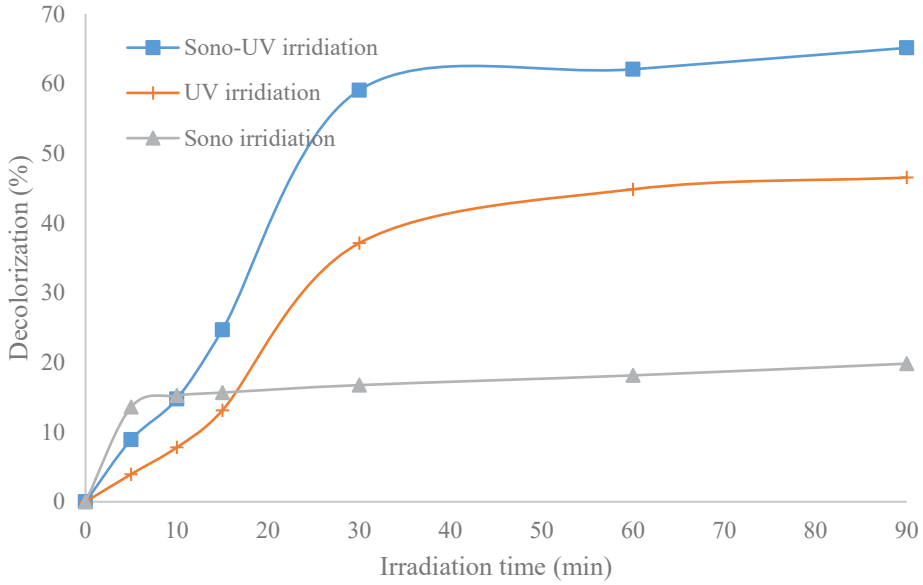

(a)

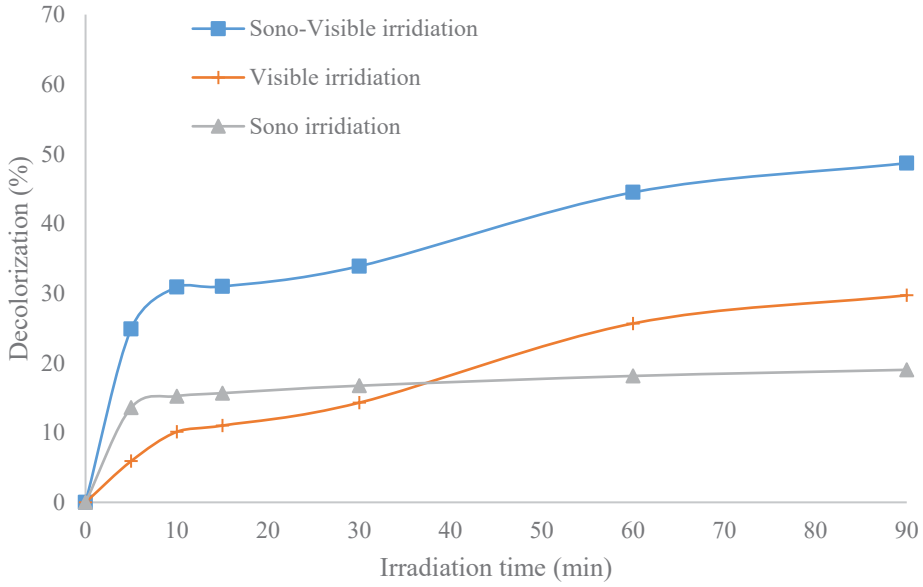

(b)

Fig. 7. The sono, photo and sono-photocatalytic activities of undoped (a) and Co-doped (b) TiO2

GRANT SUPPORT DETAILS

The present research did not receive any financial support.

CONFLICT OF INTEREST

The authors declare that there is not any conflict of interests regarding the publication of this manuscript. In addition, the ethical issues, including plagiarism, informed consent, misconduct, data fabrication and/ or falsification, double publication and/or submission, and redundancy has

been completely observed by the authors.

LIFE SCIENCE REPORTING

No life science threat was practiced in this research.

CONCLUSION

This study investigates the synthesis and characterization of co-doped TiO_2 nanoparticles with Zn, Fe, and Mg elements, and their enhanced photocatalytic activity for methyl orange degradation. The XRD patterns confirm the anatase phase of TiO_2, while SEM images reveal spherical nanoparticles with increased size after co-doping. EDX analysis verifies the successful incorporation of Zn, Fe, and Mg elements into the TiO_2 lattice. The UV-vis spectra show a red shift in the absorption spectra, indicating alterations in the crystal structure and electronic characteristics of the co-doped TiO_2. The band gap energy is reduced to 2.60 eV, enabling the absorption of visible light and generation of reactive oxygen species. The co-doped TiO_2 exhibits significantly improved sono-photocatalytic activity under both UV and visible light irradiation, achieving degradation rates of 60.1% and 48.7%, respectively. The enhanced activity is attributed to the increased diameter and crystallite size, reduced band gap, and increased surface active sites. This study demonstrates a higher efficiency compared to previous investigations, highlighting the potential of co-doped TiO_2 nanoparticles for environmental remediation applications.

REFERENCES

Abza, T., Saka, A., Tesfaye, J. L., Gudata, L., Nagaprasad, N., & Krishnaraj, R. (2022). Synthesis and Characterization of Iron Doped Titanium Dioxide (Fe: TiO2) Nanoprecipitate at Different pH Values for Applications of Self-Cleaning Materials. Advances in Materials Science and Engineering, 2022(1), 2748908.

Akhter, P., Arshad, A., Saleem, A., & Hussain, M. (2022). Recent development in non-metal-doped titanium dioxide photocatalysts for different dyes degradation and the study of their strategic factors: a review. Catalysts, 12(11), 1331

Alalwan, H. A., Ali, N. S. M., Mohammed, M. M., Mohammed, M. F., & Alminshid, A. H. (2023). A comparison study of methyl green removal by peroxi-coagulation and peroxi-electrocoagulation processes. Cleaner Engineering and Technology, 13, 100623.

Chen, Z., Yu, S., Liu, J., Zhang, Y., Wang, Y., Yu, J., ... & Zhang, J. (2023). C, F co-doping Ag/TiO2 with visible light photocatalytic performance toward degrading Rhodamine B. Environmental Research, 232, 116311.

Cheng, X., Yu, X., & Xing, Z. (2012). One-step synthesis of Fe–N–S-tri-doped TiO2 catalyst and its enhanced visible light photocatalytic activity. Materials Research Bulletin, 47(11), 3804-3809.

Darwish, A. M., Asiri, A. M., & Mahboob, M. (2021). Recent advances in iron-doped titanium dioxide photocatalysts for environmental applications. Journal of Environmental Management, 284, 111951.

Dozzi, M. V., & Selli, E. (2013). Doping TiO2 with p-block elements: Effects on photocatalytic activity. Journal of Photochemistry and Photobiology C: Photochemistry Reviews, 14, 13-28.

Fagan, R., McCormack, D. E., Dionysiou, D. D., & Pillai, S. C. (2016). A review of solar and visible light active TiO2 photocatalysis for treating bacteria, cyanotoxins and contaminants of emerging concern. Materials Science in Semiconductor Processing, 42, 2-14.

Ganesan, P., Gantepogu, C. S., Duraisamy, S., Valiyaveettil, S. M., Tsai, W. H., Hsing, C. R., ... & Wu, M. K. (2024). Carrier optimization and reduced thermal conductivity leading to enhanced thermoelectric performance in (Mg, S) co-doped AgSbTe2. Materials Today Physics, 42, 101358.

Ghorbanpour, M., & Feizi, A. (2019). Iron-doped TiO2 catalysts with photocatalytic activity. Journal of Water and Environmental Nanotechnology, 4(1), 60-66.

Ghorbanpour, M., & Feizi, A. (2020). Application of synthesizing tri-metallic Zn and Ag co-doped TiO2 nano-photocatalyst by a one-step synthesis technique in treating water pollutants. Desalination and Water Treatment, 200, 187-195.

Gogate, P. R. (2020). Improvements in catalyst synthesis and photocatalytic oxidation processing based on the use of ultrasound. Heterogeneous Photocatalysis: Recent Advances, 71-105.

Jabbari, V., Hamadanian, M., Reisi-Vanani, A., Razi, P., Hoseinifard, S. and Villagran, D., 2015. In, V-Co-doped TiO 2 nanocomposite prepared via a photochemical reduction technique as a novel high efficiency visible-light-driven nanophotocatalyst. *RSC advances*, *5*(95), pp.78128-78135.

Kunnamareddy, M., Diravidamani, B., Rajendran, R., Singaram, B., & Varadharajan, K. (2018). Synthesis of silver and sulphur codoped TiO 2 nanoparticles for photocatalytic degradation of methylene blue. Journal of Materials Science: Materials in Electronics, 29, 18111-18119.

Luu, T. V. H., Nguyen, H. Y. X., Nguyen, Q. T., Nguyen, Q. B., Nguyen, T. H. C., Pham, N. C., ... & Dao, N. N. (2024). Enhanced photocatalytic performance of ZnO under visible light by co-doping of Ta and C using hydrothermal method. RSC advances, 14(18), 12954-12965.

Liu, X., Wu, Z., Zhang, Y., & Tsamis, C. (2019). Low temperature Zn-doped TiO2 as electron transport layer for 19% efficient planar perovskite solar cells. *Applied Surface Science*, *471*, 28-

Madadi, M., Ghorbanpour, M., & Feizi, A. (2018). Antibacterial and photocatalytic activity of anatase phase Ag-doped TiO2 nanoparticles. Micro & Nano Letters, 13(11), 1590-1593.

Madadi, M., Ghorbanpour, M., & Feizi, A. (2019). Preparation and characterization of solar light-induced rutile Cu-doped TiO2 photocatalyst by solid-state molten salt method. Desalination and Water Treatment, *145*, 257-261.

Maki, L. K., Maleki, A., Rezaee, R., Daraei, H., & Yetilmezsoy, K. (2019). LED-activated immobilized Fe-Ce-N tri-doped TiO2 nanocatalyst on glass bed for photocatalytic degradation organic dye from aqueous solutions. Environmental Technology & Innovation, 15, 100411.

Mancuso, A., Navarra, W., Sacco, O., Pragliola, S., Vaiano, V., & Venditto, V. (2021). Photocatalytic degradation of thiacloprid using tri-doped tio2 photocatalysts: A preliminary comparative study. Catalysts, 11(8), 927.

Na-Phattalung, S., Harding, D. J., Pattanasattayavong, P., Kim, H., Lee, J., Hwang, D. W., ... & Yu, J. (2022). Band gap narrowing of TiO2 nanoparticles: A passivated Co-doping approach for enhanced photocatalytic activity. Journal of Physics and Chemistry of Solids, 162, 110503.

Nisar, S. S., Arun, S., Toan, N. K., Ahn, S. G., & Choe, H. C. (2024). Formation of Ca, P, and Zn-doped ZrO2/TiO2 coating layer via plasma electrolytic oxidation and magnetic sputtering: Improving surface characteristics and biocompatibility of Ti–6Al–4V alloy. Journal of Materials Research and Technology, 31, 1282-1303.

Peiris, S., de Silva, H. B., Ranasinghe, K. N., Bandara, S. V., & Perera, I. R. (2021). Recent development and future prospects of TiO2 photocatalysis. Journal of the Chinese Chemical Society, 68(5), 738-769.

Rehan, A. I., Rasee, A. I., Awual, M. E., Waliullah, R. M., Hossain, M. S., Kubra, K. T., ... & Awual, M. R. (2023). Improving toxic dye removal and remediation using novel nanocomposite fibrous adsorbent. Colloids and Surfaces A: Physicochemical and Engineering Aspects, 673, 131859.

Sewnet, A., Abebe, M., Asaithambi, P., & Alemayehu, E. (2022). Visible-light-driven g-C3N4/TiO2 based heterojunction nanocomposites for photocatalytic degradation of organic dyes in wastewater: a review. Air, Soil and Water Research, 15, 11786221221117266.

Sari, F. N. I., Saputro, B. W., & Ting, J. M. (2023). Structural and defect modulations of co-precipitation synthesized high-entropy Prussian blue analogue nanocubes via Cu/Zn co-doping for enhanced electrochemical performance. Journal of Materials Chemistry A, 11(36), 19483-19495.

Umare, S.S., Charanpahari, A. and Sasikala, R., 2013. Enhanced visible light photocatalytic activity of Ga, N and S Co-doped TiO2 for degradation of azo dye. Materials Chemistry and Physics, 140(2-3), pp.529-534.

Waliullah, R. M., Rehan, A. I., Awual, M. E., Rasee, A. I., Sheikh, M. C., Salman, M. S., ... & Awual, M.

R. (2023). Optimization of toxic dye removal from contaminated water using chitosan-grafted novel nanocomposite adsorbent. Journal of Molecular Liquids, 388, 122763.

Xu, Y., Wang, Y., & Zhang, T. (2020). A review on the visible-light photocatalytic applications of iron-doped titanium dioxide. Materials Today Sustainability, 8, 100027.

Yihunie, M. T. (2024). Enhanced photoluminescence and structural properties of Zn-doped anatase TiO2 nanoparticles. Materials Research Express, 11(7), 075007.

Zhang, H., Liang, Y., Wu, X., & Zheng, H. (2012). Enhanced photocatalytic activity of (Zn, N)-codoped TiO2 nanoparticles. Materials Research Bulletin, 47(9), 2188-2192.

Zhang, H., Watanabe, A., & Zhang, Q. (2019). Sonophotocatalytic processes for the treatment of wastewater. Water Research, 161, 401-410.